ISSSD 2022

XXII INTERNATIONAL SYMPOSIUM ON SOLID STATE DOSIMETRY

Proceedings

Vol. 1

Hybrid
September 19 to 23, 2022

Organizing Institutions

Casa abierta al tiempo

UNIVERSIDAD AUTÓNOMA DE ZACATECAS
FRANCISCO GARCÍA SALINAS

ININ

FEDERACIÓN DE RADIOPROTECCIÓN DE AMÉRICA LATINA Y EL CARIBE
FRALC

Investigation of dosimetric properties of $CaSO_4$:Mn phosphor prepared using slow evaporation route

Anderson M. B. Silva [1 *], Daniel S. Rodrigues[1], Patrícia L. Antonio[2], Danilo O. Junot [3], Linda V.E. Caldas[2], Divanizia N. Souza[1]

[1] Departamento de Física, Universidade Federal de Sergipe, Marechal Rondon, S/N, 49.100-000, São Cristovão, SE, Brazil

[2] Instituto de Pesquisas Energéticas e Nucleares, Comissão Nacional de Energia Nuclear, IPEN/CNEN-SP, Av. Prof. Lineu Preste, 2242, 05508-000, São Paulo, SP, Brazil

[3] Instituto de Física Armando Dias Tavares, Universidade do Estado do Rio de Janeiro UERJ, Rua São Francisco Xavier, 524, 20550-013, Rio de Janeiro, RJ, Brazil

[*]Email: andersonmanoel22@hotmail.com

Abstract

The objective of this work was to investigate the luminescent properties of $CaSO_4$:Mn synthesized by slow evaporation route. The crystalline structure, morphology, thermal and optical properties of the phosphors were characterized by X-ray diffraction analysis (XRD), Scanning electron microscopy (SEM), photoluminescence (PL) and thermogravimetric analysis (TGA). Moreover, using thermoluminescence (TL) and optically stimulated luminescence (OSL) techniques, the dosimetric properties of the phosphors, such as emission spectra, glow curve reproducibility, dose-response linearity, fading of the luminescent signal, variation of the TL intensity with the heating rate, OSL decay curves, correlation between TL and OSL emissions and minimum detectable dose (MDD) were comprehensively investigated. For dosimetric analyses, the samples were irradiated with doses from 169 mGy to 10 Gy. The emission band fits with the characteristic line of the Mn^{2+} emission features, ascribed to $^6A_1 \rightarrow {}^4T_1$ transition. $CaSO_4$:Mn pellets present a TL glow curve with a single typical peak centered around 494 nm, an OSL decay curve with predominance of a fast decay component, and a MDD on the order of hundreds of mGy. The luminescent signals showed to be linear and reproducible in the studied dose range. The trapping centers located between 0.83 eV and 1.07 eV were revealed for different heating rates in the TL study. The high TL sensitivity of $CaSO_4$:Mn was proven when comparing with commercially available dosimeters. The luminescent signals exhibit a smaller fading than described in the literature for $CaSO_4$:Mn produced by other methods.

Keywords: dosimetric properties; slow evaporation route; thermoluminescence; optically stimulated luminescence; $CaSO_4$: Mn.

1.-INTRODUCTION

Manganese divalent (Mn^{2+}) ions are significant transition metal activators for broadband and wavelength-tunable luminescence due to the d-d electronic transitions and the interactions with $3d^5$ electronic configuration [Liu *et al.*, 2017].

In recent decades, these ions have attracted considerable attention due to their applications in many technological fields, such as in biomedical imaging and labelling [Song *et al.*, 2015], magnetic sensors [Raghuwanshi *et al.*, 2014], displays [Wang *et al.*, 2014], lasers [Du *et al.*, 2021], photovoltaic applications [Zhou *et al.*, 2015] and optical data storage [Lin *et al.*, 2020]. Moreover, the development and study of luminescence of synthetic materials subsidized with manganese ions for radiation dosimetry application have been for many years investigated and are still intensively researched, primarily for use in thermoluminescent (TL) and optically stimulated luminescent (OSL) dosimetry [Bahl *et al.*, 2017; Luchechko *et al.*, 2019; Menon *et al.*, 2005; Oberhofer and Scharmann 1993; Yamashita *et al.*, 1970; Zahedifar *et al.*, 2011].

From the host material point of view, calcium sulphate ($CaSO_4$) activated with manganese was the first investigated synthetic material to be used as thermally stimulated luminescence dosimeter [Bahl *et al.*, 2017]. Despite this fact, $CaSO_4$:Mn attracted attention because of its outstanding sensitivity [Watanabe 1951]; its use was limited due to a simple reason that its TL glow curve presented a single peak centered at 100°C and considerable fading of the TL signal (40–85% in the first 3 days after the irradiation) [Oberhofer and Scharmann 1993].

For the purpose of expanding the supply of viable solid-state detectors, a large number of methods were commonly used for the preparation of $CaSO_4$ powders, such as the co-precipitation method [Nuraeni *et al.*, 2019], recrystallization method [Bahl *et al.*, 2017], sol-gel method [Kadari *et al.*, 2016], hydrothermal method [Zahedifar *et al.*, 2011], solid state reaction route [Rani *et al.*, 2015] and slow evaporation route [Yamashita *et al.*, 1970].

Thereby, according to the antecedents mentioned above, in this work the Yamashita method [Yamashita *et al.*, 1970] was employed, a well-known slow evaporation route, but with some adjustment in the circuit (controlled air atmosphere, an improved distillation system, and fully isolated from the external environment), which was improved by Junot *et al.*, [2016].

This study is focused on the preparation and investigation of TL and OSL properties of $CaSO_4$:Mn synthesized by the slow evaporation route, since the production route used by our research group showed efficiency in the growth of other crystals, such as $CaSO_4$:Tb,Eu [Junot *et al.*, 2016], $CaSO_4$:Tm and $CaSO_4$:Tm,Ag [Junot *et al.*, 2019], $CaSO_4$:Tb, $CaSO_4$:Tb,Ag and $CaSO_4$:Tb,Ag(NP) [Silva *et al.*, 2020] and $CaSO_4$:Mn,Tb [Silva *et al.*, 2022].

2.- MATERIALS AND METHODS

2.1. Sample preparation

The $CaSO_4$:Mn crystals were prepared using a slow evaporation method from a mixture of calcium carbonate ($CaCO_3$) (Merck, 99%), sulfuric acid (H_2SO_4) (Vetec, 95-99%) and manganese nitrate ($Mn(NO_3)_2 * 4H_2O$) with a concentration value of 0.1 mol%. The parameters to obtain $CaSO_4$:Mn crystals were established in previous works [Junot *et al.*, 2016; Junot *et al.*, 2019; Silva *et al.*, 2020; Silva *et al.*, 2022].

After the sulfuric acid evaporation, the $CaSO_4$:Mn crystals were washed, ground, and sieved. The resulting powder was calcined for 1 hour at 600 °C. Thereafter, the powder was mixed uniformly with polytetrafluoroethylene (Teflon), in a proportion of 2:1. After a uniaxial pressure of 0.5 tons during 10 s, pellets of (40±1) mg, 6 mm in diameter and approximately 1 mm thickness were produced. Finally, the pellets were sintered at 450 °C for 1 h.

2.2. Sample characterization

X-ray diffraction (XRD) pattern was recorded using Cu-target (Cu-K_α = 1.54 Å) on Rigaku diffractometer (RINT 2000/PC). The phase identification was performed using the International Center for Diffraction Data (ICDD) PDF 00-037-1496. Scanning electron microscopy (SEM) images were recorded using a Hitachi TM-3000 scanning microscope with carbon substrate. The excitation and emission spectra were obtained using a JASCO FP8600 spectrofluorometer. The thermal behavior was investigated using thermogravimetric analysis (TGA) with a type Shimadzu-50 instrument, at a heating rate of 10 °C/min with N_2 as a carrier gas at a flow rate of 50 cm^3/min.

TL and OSL measurements were carried out using a Risø TL/OSL-DA-20 automatic Reader. The samples were irradiated with a beta source (dose rate of 81.6 mGy/s), which is coupled to the Riso system. In order to carry out measurements of the TL emission spectra, a high resolution spectrometer from Ocean Optics was coupled in place of the photomultiplier. This reader has a Hoya U-340 (340 ± 40) nm filter. For the analysis of the heating rate on the TL emission, the pellets were exposed to heating rates varying from 1 °C/s up to 10 °C/s, to a maximum temperature of 400 ºC. For all other measurements, the heating rate was kept at 10 °C/s. Glow curve deconvolutions and TL kinetic parameters wereobtained by means of OriginLab 8.0 software (OriginLab Co., USA). The TL curve wasfitted using the equation for the general kinetic order presented by Chen and McKeever [1997], to determine the kinetic order (b), activation energy (E) and frequency factor (s) parameters of the TL peaks.

In the TL sensitivity analysis, five commercial dosimeters were used for comparison with $CaSO_4$:Mn: $CaSO_4$:Dy (produced at the Dosimetric Materials Laboratory of IPEN), LiF:Mg,Ti (Harshaw TLD-100), CaF_2:Dy (Harshaw TLD-200), CaF_2:Mn (Harshaw TLD-400) and $CaSO_4$:Dy (Harshaw TLD-900). All the pellets were pre-irradiated to 169 mGy with a beta radiation source ($^{90}Sr/^{90}Y$) and the glow curves read immediately using Hoya U-340 (340 ± 40) nm filter.

For the OSL readings, the signal was collected over 40 seconds and the samples were stimulated with blue LEDs (with emission at 470 nm), in continuous-wave mode. The

experimental OSL decay curves composed by three first-order exponential decay functions were obtained by fitting using the following Equation (1):

$$I_{OSL} = A_1\, e^{-t/\tau_1} + A_2\, e^{-t/\tau_2} + A_3\, e^{-t/\tau_3} \qquad (1)$$

where I_{OSL} is the total OSL intensity; A_1, A_2, and A_3 are constant coefficients and τ_1, τ_2, and τ_3 are the decay constants related to the different sets of traps [Valença *et al.*, 2018].

The minimum detectable dose (MDD) of the luminescent signal of the produced samples was calculated by the Equation (2) proposed by Oberhofer e Scharmann [1981].

$$MDD = (\bar{B} + 3\sigma_{\bar{B}})f_c \qquad (2)$$

Where $\bar{B}$ is the average of the TL or OSL response of the non-irradiated dosimeters, $\sigma_{\underline{B}}$ is the standard deviation of the readings of non-irradiated dosimeters, and f_c is a calibration factor calculated from the inverse of the slope of the line of TL/OSL response to absorbed dose. After the TL/OSL measurements, the pellets were thermally treated at 400 °C for 2 h, for reutilization.

3.- RESULTS AND DISCUSSION

3.1. Structural characterization

Figure 1 shows the XRD pattern of synthesized $CaSO_4$:Mn samples. As can be seen, the diffraction peaks agree with those of $CaSO_4$ anhydrite (ICDD 00-037-1496) pattern to a crystal of orthorhombic symmetry [Silva *et al.*, 2021], whose reference lines are included for comparison. The results revealed that the obtained samples showed pure phase and there is no evidence of presence of the dopants due to their low concentrations (≤ 0.1% mol).

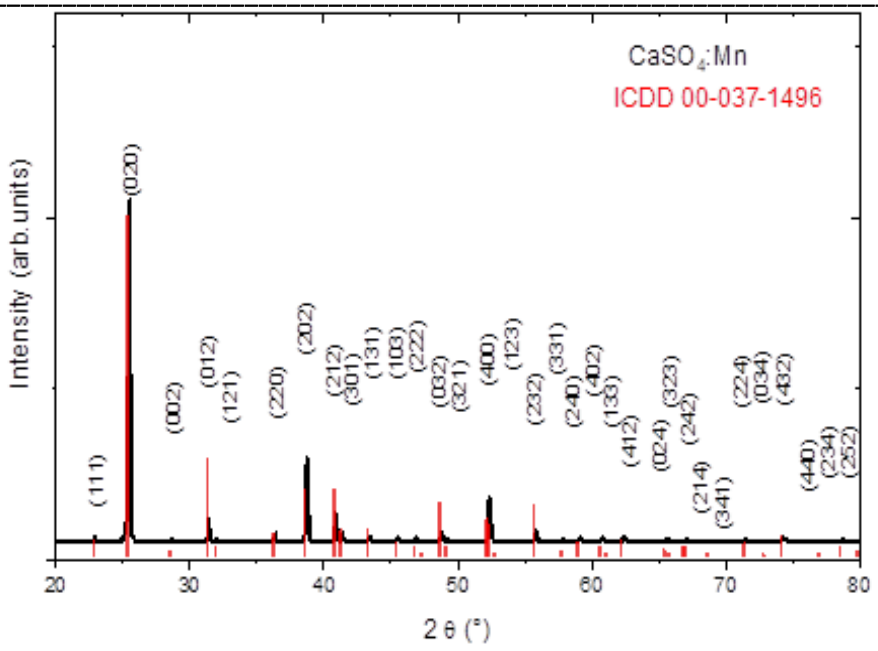

Figure 1. Experimental X-ray diffractogram of $CaSO_4$:Mn powder, presented with its crystallographic pattern and standard Bragg reflections.

3.2. Scanning electron microscopy (SEM)

The main features on the surface of crystalline $CaSO_4$:Mn are depicted in the SEM micrograph in Figure 2. The $CaSO_4$ samples obtained after calcination of the compound show well grained images with quite agglomeration in the grains with average crystal dimensions of <150 µm.

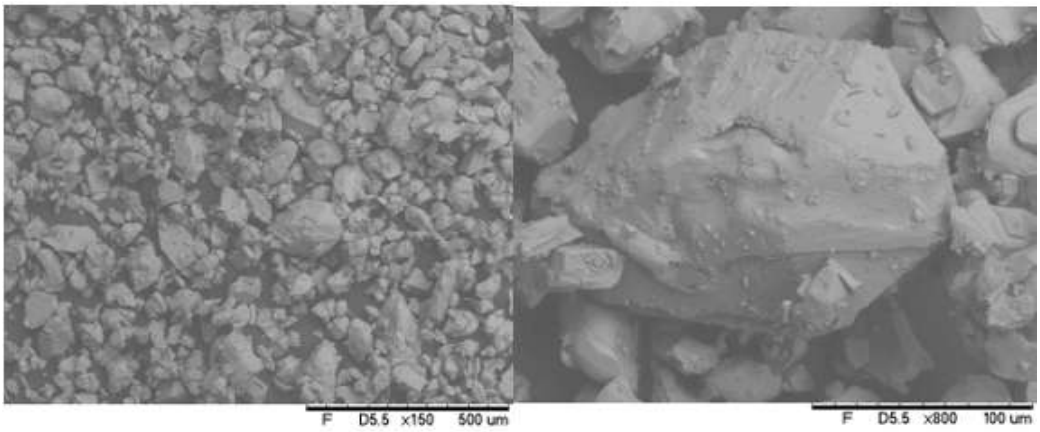

Figure 2. SEM images of $CaSO_4$:Mn.

3.3. Photoluminescence studies

The photoluminescence spectrum of the $CaSO_4$:Mn phosphor is shown in Figure 3. The spectrum was monitored at an excitation wavelength at 398 nm, showing a broad band around 494 nm, attributable to contributions of Mn^{2+} in the host lattice. The green emission observed is typical for bivalent manganese ions, in four-fold regular tetrahedral coordination, and corresponds to the $^4T_1 \rightarrow {}^6A_1$ transition in Mn^{2+} ion [Luchechko *et al.*, 2019; Menon *et al.*, 2005; Zahedifâr *et al.*, 2011].

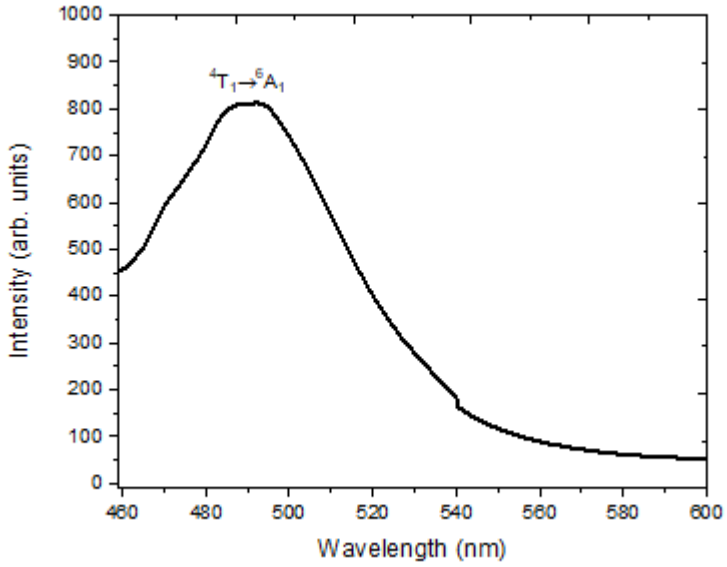

Figure 3. Emission spectra of $CaSO_4$:Mn excited with 398 nm.

3.4 Thermogravimetric analysis (TGA)

The thermal behaviors of the $CaSO_4$ powder were determined by thermogravimetric analysis (TGA) as shown in Figure 4. There is a weight loss of only 1% if the samples are annealed up to 450 °C, and a 20.3% further weight loss on annealing up to 1000 °C. This shows that the temperature used for sintering the pellets at 450°C for 1 h is adequate since there is no major weight loss, indicating an absence of additional structural changes in this region.

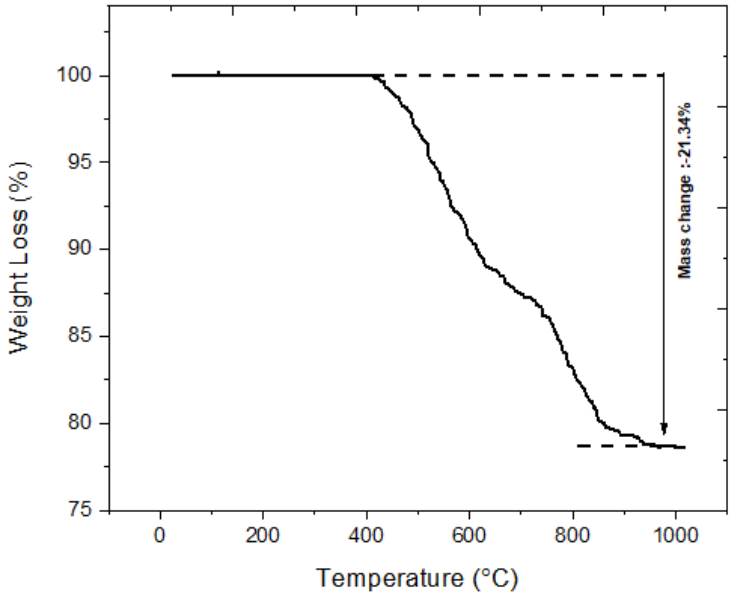

Figure 4. TGA curves of the as-prepared samples.

3.5 Thermoluminescent studies

3.5.1 TL emission spectra

The 3D TL emission spectra of $CaSO_4$:Mn irradiated with 50 Gy are shown in Figure 5(a) and 5(b). The glow curve for $CaSO_4$:Mn presented a single peak centered at approximately 150°C, around 494 nm. The wavelength of the emission is consistent with the literature report for Mn^{2+} ions [Luchechko *et al.*, 2019; Menon *et al.*, 2005; Zahedifar *et al.*, 2011]. This observed transition corresponds to the $^6A_1 \rightarrow {}^4T_1$ which confirms the incorporation of the Mn^{2+} ion into the calcium sulphate matrix.

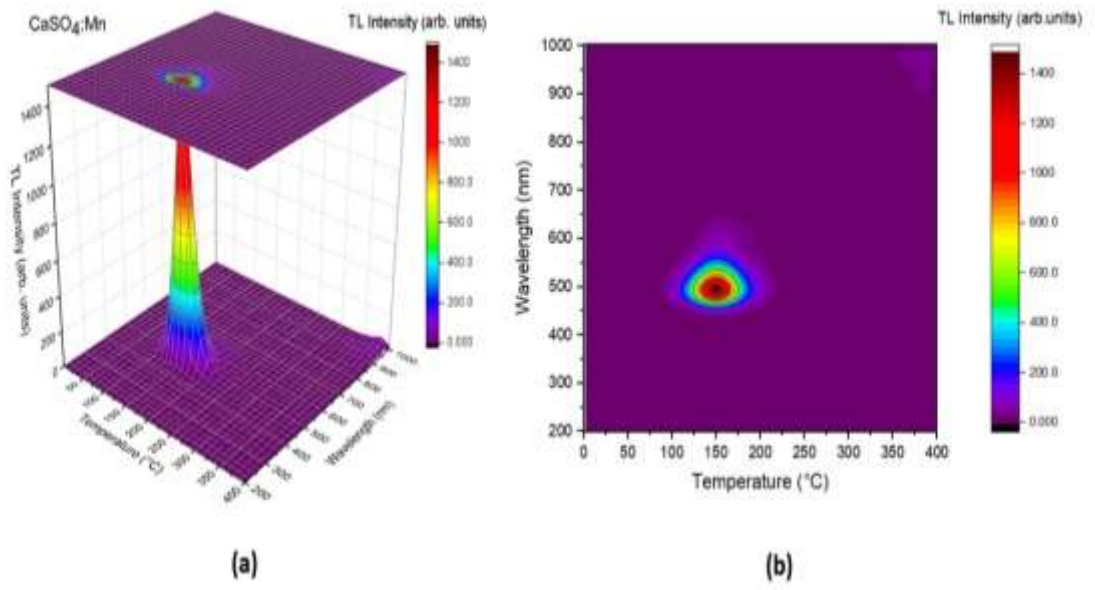

Figure 5. (a) Isometric 3D-TL emission plot from $CaSO_4$:Mn phosphor and (b) $CaSO_4$:Mn TL emission spectrum couture diagram.

Once the peak wavelength is determined, the TL peak for the $CaSO_4$:Mn produced by the evaporation route was found to appear around 150 °C. This showed a large advantage of this material in comparison to the $CaSO_4$:Mn materials reported in the literature, since higher temperature peaks seems to be more stable than lower temperature ones. It is worth mentioning that there is a divergence in the TL emission curve when samples are produced by different synthesis methods. Examples of this variation were reported by Bahl *et al.* [2017]. They obtained by the recrystallization method one glow curve for the $CaSO_4$:Mn with a single peak at around 110 °C.

Zahedifara *et al.*[2011] synthesized this material by the hydrothermal method and they identified one complex glow curve with three overlapping peaks, while by method of Yamashita *et al.* [1970], this glow curve of $CaSO_4$:Mn presented a simple form and a peak at 100°C.

3.5.2 Variation in the heating rate

The effect of the heating rate on the thermoluminescence of the $CaSO_4$:Mn phosphors was examined. Figure 6(a) shows TL responses of the samples readout at different heating rates after being irradiated with 169 mGy of a $^{90}Sr/^{90}Y$ beta source. Increasing the heating rate of the sample from 1.0°C/s to 10°C/s a TL peak shift to higher temperatures was observed, Figure 6(b), as well as a decrease of the peak height. This observation may be explained based on the phenomenon of thermal quenching, which takes place inside the phosphor and causes the decrease of luminescence efficiency due to the increased probability of non-radiative transitions [Kadari and Kadri 2015].

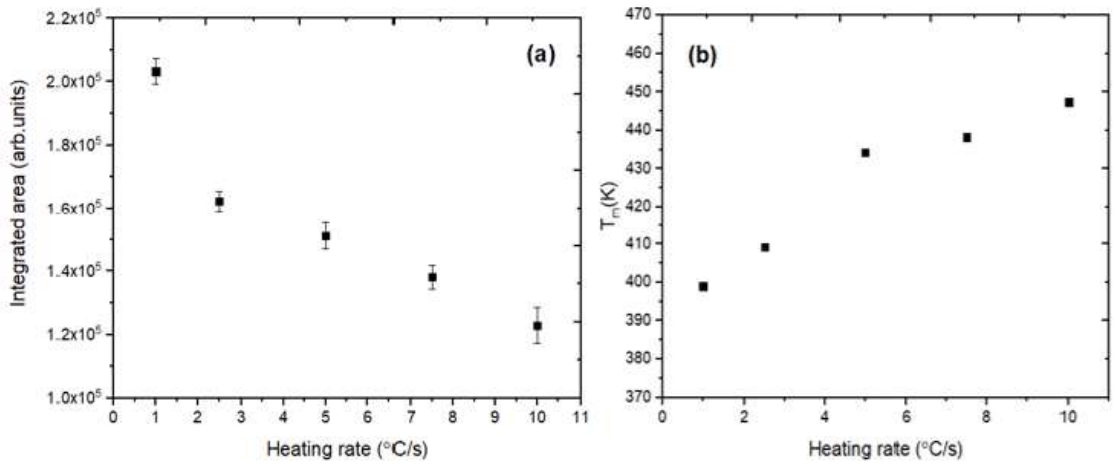

Figure 6. (a) TL intensity of $CaSO_4$:Mn samples exposed to the same absorbed dose and measured at different heating rates and (b) peak temperatures (T_m) vs. heating rate.

Table 1 shows the TL parameters obtained by employing the general kinetic order fitting on TL glow curves of $CaSO_4$:Mn for different heating rates. The peak temperatures (T_m), the maximum peak intensities (I_m), the kinetic order value (b), the activation energies (E) and the frequency factor (s) were determined.

Table 1. Parameters of the TL glow curve of $CaSO_4$:Mn obtained by employing the general kinetic order equation [Chen and McKeever 1997].

Heating rates (°C/s)	T_m (K)	I_m (arb. units)	b (kinetic order)	E (eV)	s (s^{-1})
1.0	399.01 ± 0.36	5434.2 ± 49.68	1.93±0.12	0.83±0.01	$4.69x10^{11}$
2.5	409.24 ± 0.20	4651.77 ± 38.55	1.95 ± 0.03	0.914± 0.01	$2.93x10^{12}$
5	434.26 ± 0.20	4100.27 ± 38.56	1.96 ± 0.04	0.97 ± 0.02	$2.84x10^{12}$
7.5	438.20 ± 0.19	3946.37 ± 19.72	1.97 ± 0.03	1.01 ± 0.01	$6.69x10^{12}$
10	447.32 ± 0.15	3541.6 ± 19.21	1.98 ± 0.03	1.07 ± 0.01	$1.86x10^{13}$

The TL emission glow curves for the $CaSO_4$:Mn samples showed one peak varying between 399 K and 447 K for different heating rates. The trapping centers located between 0.83 and 1.07 eV were revealed. The order of kinetics was found to be between one and two, indicating the existence of a general order of kinetics in the TL process.

Since a heating rate of 10 °C/s is usually employed in standard dosimetry, in this work it is preferred to maintain this heating rate for all the consecutive TL dosimetric characterizations.

3.5.3. TL Reproducibility, Fading and Linearity.

In order to evaluate whether the luminescence signal of the $CaSO_4$:Mn pellets is reproducible, five cycles of annealing - irradiation with 169 mGy - reading were performed. As observed in Figure 7, the results show an adequate reproducibility, with the average value of the coefficient of 6.22 % for $CaSO_4$:Mn samples, meeting the requirements of the ISO 12794 [ISO 2000], which states that this C.V% should not exceed 10%. Hence, the result confirmed that these pellets may be reusable in systemic radiation dose assessment.

The ratio of the TL response of each dosimeter to the mean batch response of all dosimeters results in the homogeneity coefficient (C_H%), and the average value of 3.15% was obtained.

The fading of this phosphor was evaluated up to 28 days after irradiation. Figure 8 shows normalized TL of the pellets, previously irradiated with 169 mGy, and then being stored over a period of one day, 7 days, 14 days, 21 days and 28 days at room temperature and under light protection. The total integrated area of the glow curves exhibited the following reduction of its original value: 14 % in 1 day, 46% in 7 days, 64 % in 14 days, 69% in 21 days and 75% after 30 days.

The $CaSO_4$:Mn prepared using slow evaporation route minimized the fading behavior, when compared to those reported in the literature. Bahl *et al.* [2017] and Menon *et al.* [2005] reported a fading of the TL intensity of this material very considerable of 40-85% in the first 3 days after radiation exposure. This peak shift to 150 ºC in comparison to the 100 ºC peak reported, evidences the existence of more deep trap (electrons or holes trapped at deep localized trap states) and stable traps at all levels.

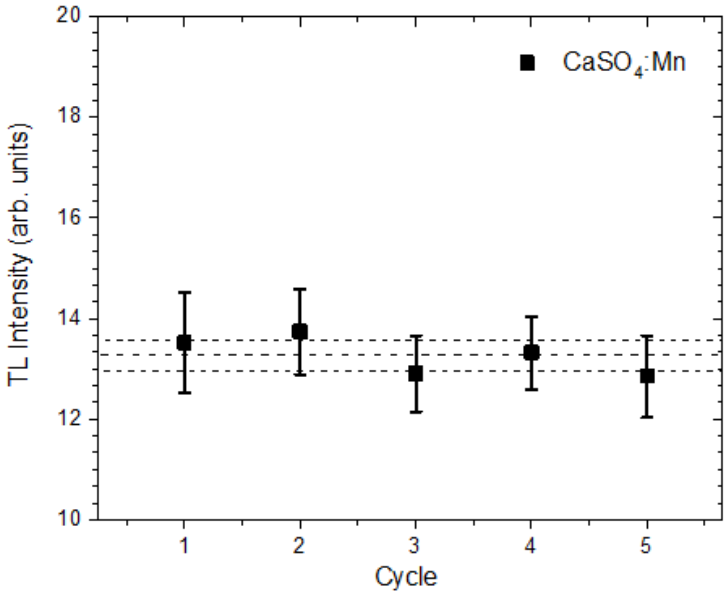

Figure 7. TL reproducibility of the $CaSO_4$:Mn samples after five cycles of the annealing - irradiation - reading procedure.

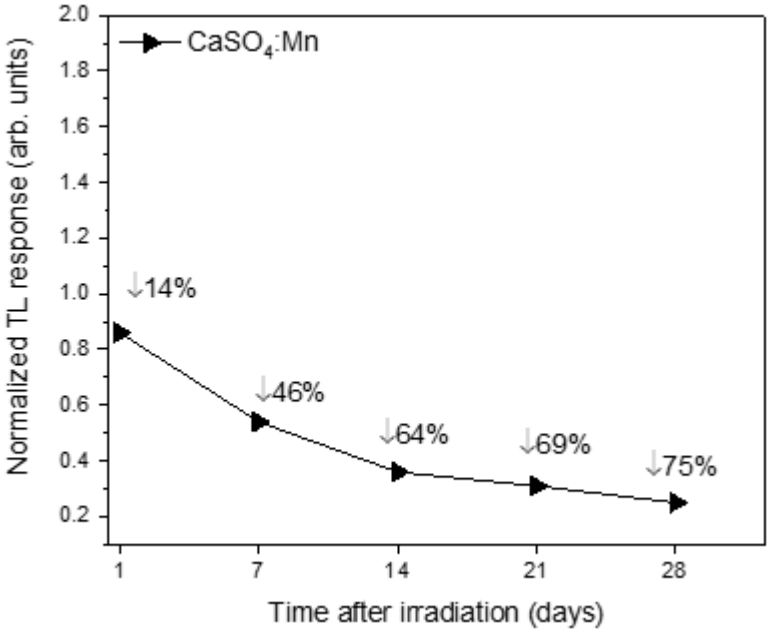

Figure 8. Normalized TL response of $CaSO_4$:Mn samples, presented with fading percentage in different storage time intervals, after a previous irradiation with 169 mGy ($^{90}Sr/^{90}Y$).

The dose-response curve of the $CaSO_4$:Mn pellets irradiated with absorbed doses from 169 mGy up to 9.971 Gy is shown in Figure 9. The linear relationship between the TL response and the absorbed doses can be observed in the whole tested dose range. The linear regression for the curve has an R-squared of 0.9989.

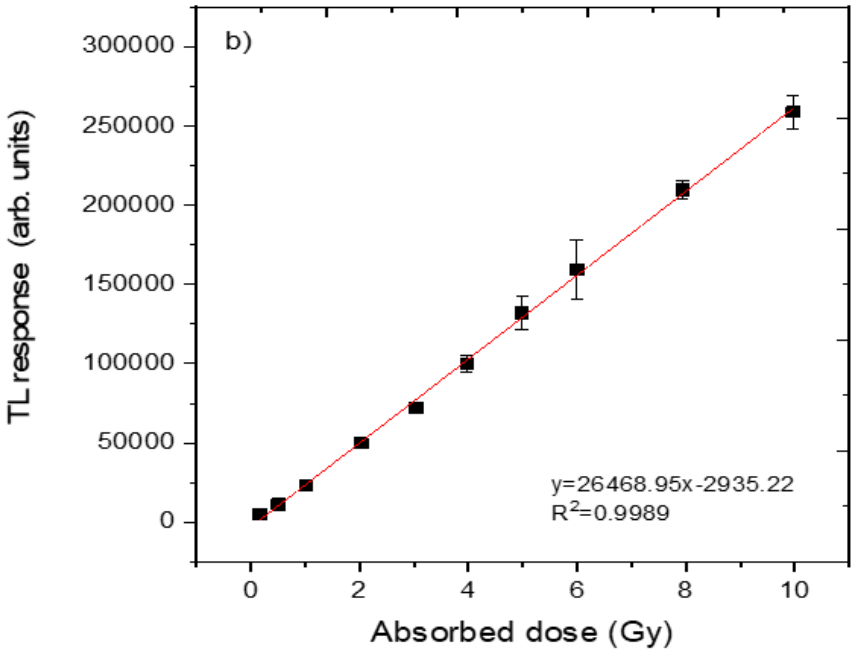

Figure 9. TL response versus absorbed dose of beta radiation ($^{90}Sr/^{90}Y$).

3.5.4 TL sensitivity

The TL sensitivity described through the TL signals intensity, per unit mass and per unit of absorbed dose ($TL*mg^{-1}*Gy^{-1}$), of the $CaSO_4$:Mn pellets produced in the present work were compared with those of the commercial dosimeters TLD-100 (LiF:Mg,Ti), TLD-200 (CaF_2:Dy), TLD-400 (CaF_2:Mn), TLD-900 ($CaSO_4$:Dy), and $CaSO_4$:Dy (IPEN) after being irradiated with absorbed doses of 169 mGy . The results indicate that the TL sensitivity of $CaSO_4$:Mn pellets was 73.7 times higher than that of TLD-400, 49.9 times higher than that of $CaSO_4$:Dy (IPEN), 23.1 times higher than that of TLD-200 and 1.79 times higher than that of TLD-900 measured in similar conditions and using Hoya U-340 (340 ± 40) nm filter. Nevertheless, this sensitivity is still lower than that usually found for high sensitivity TLD material such as TLD-100 (LiF:Mg,Ti).

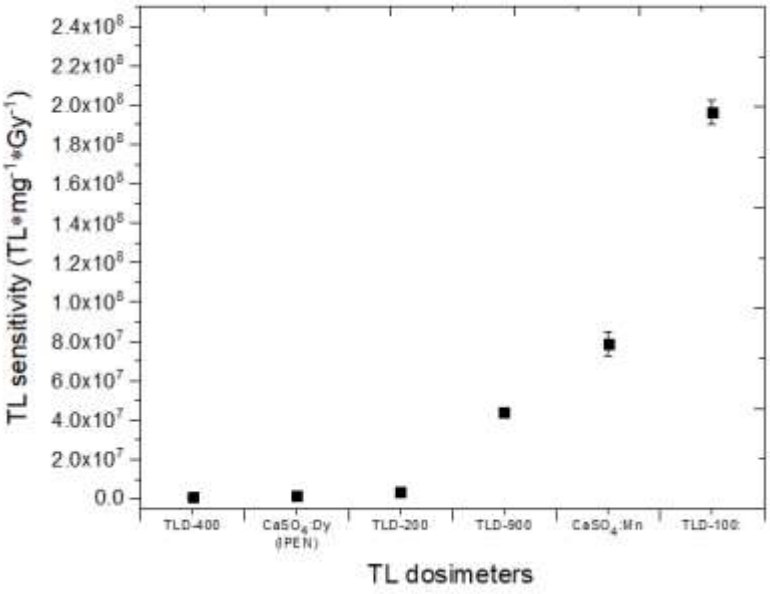

Figure 10. TL sensitivity of the $CaSO_4$:Mn samples and of commercial dosimeters irradiated with 169 mGy.

3.6 Optically stimulated luminescence studies

3.6.1. OSL decay curves

Figure 11 illustrates a fitting of the OSL decay curve obtained after 169 mGy of beta radiation dose. For this analysis, the samples were stimulated with blue light for 40 s. These exponential curves are composed of fast (blue curve), medium (orange curve) and slow (green curve) decay components. The sum of the components (red curve) is very close to the experimental OSL curve (black curve). For this was used to fitted with decaying exponential functions of Eq. (1).

The values of the constant coefficients and decay constants for each of the components are listed in Table 2. In the dose range investigated, the curves present yielded

three time constants. As presented in Table 2, the high value of A_1 confirms the predominance of a fast decay component in the experimental OSL decay curve; in this case, the emission of photons results in direct recombination between the electrons in the conduction band and the holes in the valence band of phosphor. The low value of A_3=0.085 indicates that the significance of the slow component (τ_3= 10.47) is minimal in the experimental OSL decay curve.

Table 2. The OSL parameters of the exponential fitted curves of the produced compound.

CW-OSL Component	Coefficient A_i	Decay constant t_i (s)	Exponential Fit
Fast	1.527 ± 0.014 (A_1)	0.21 ± 0.01 (t_1)	R^2: 0.9995
Medium	0.371 ± 0.009(A_2)	1.19 ± 0.02 (t_2)	
Slow	0.085 ± 0.001 (A_3)	10.47 ± 0.17 (t_3)	

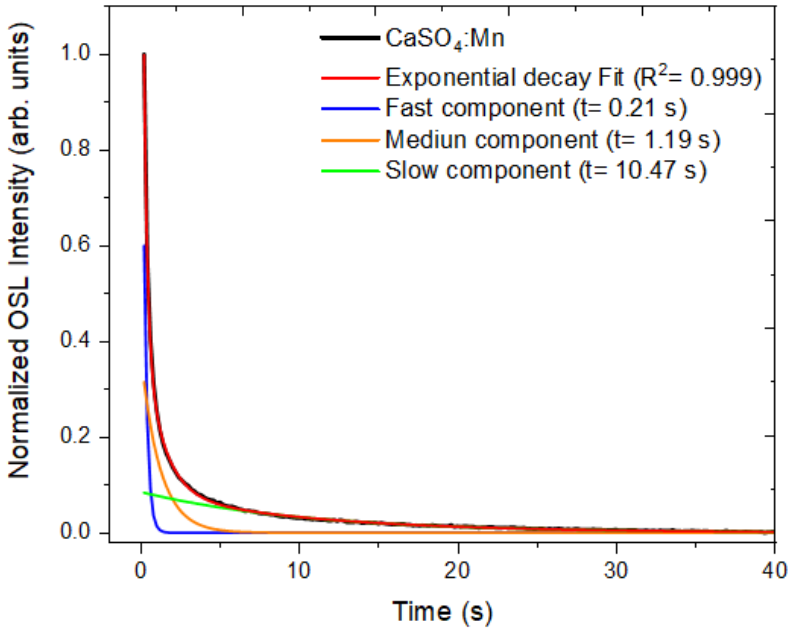

Figure 11. The CW-OSL curve and fitted OSL decay curves for samples irradiated with 169 mGy (^{90}Sr+^{90}Y).

3.6.2. OSL reproducibility

In the present study, the OSL response reproducibility of the $CaSO_4$:Mn pellets was also determined as described in Section 3.4.1 for the TL. In Figure 12 each point represents the average values of the OSL readings of 15 pellets, and the bars represent their standard deviations. The reproducibility of the OSL measurements was found to be approximately 4.14%, and for the homogeneity study , the homogeneity coefficient (C_H%) the mean value of 4.46% was obtained.

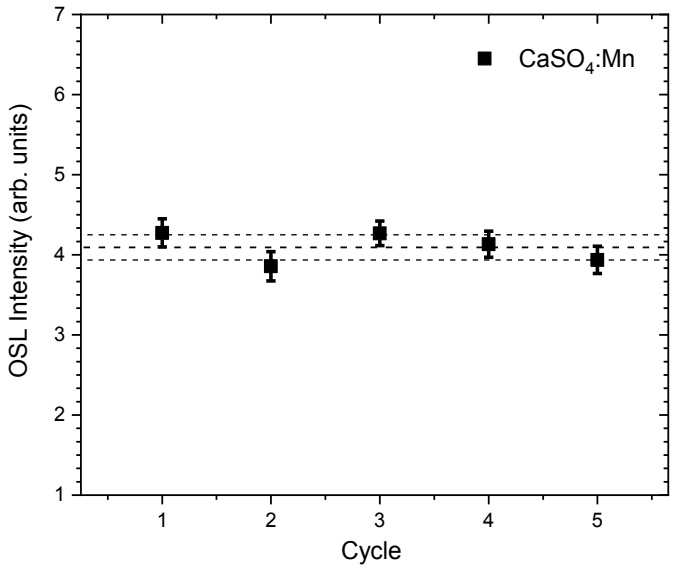

Figure 12. OSL Reproducibility of the $CaSO_4$:Mn samples after five cycles of the annealing - irradiation - reading procedure.

3.6.3. OSL dose response

Figure 13 (a) shows the OSL decay of $CaSO_4$:Mn samples exposed to the beta source from 169 mGy up to 9.971 Gy. The OSL dose-response curve is shown in Fig. 13(b). The results showed that the OSL signal is proportional to the absorbed radiation

dose, i.e., it increases with the number of trapped electrons and holes. A linear adjustment presented a linear correlation coefficient of 0.9989.

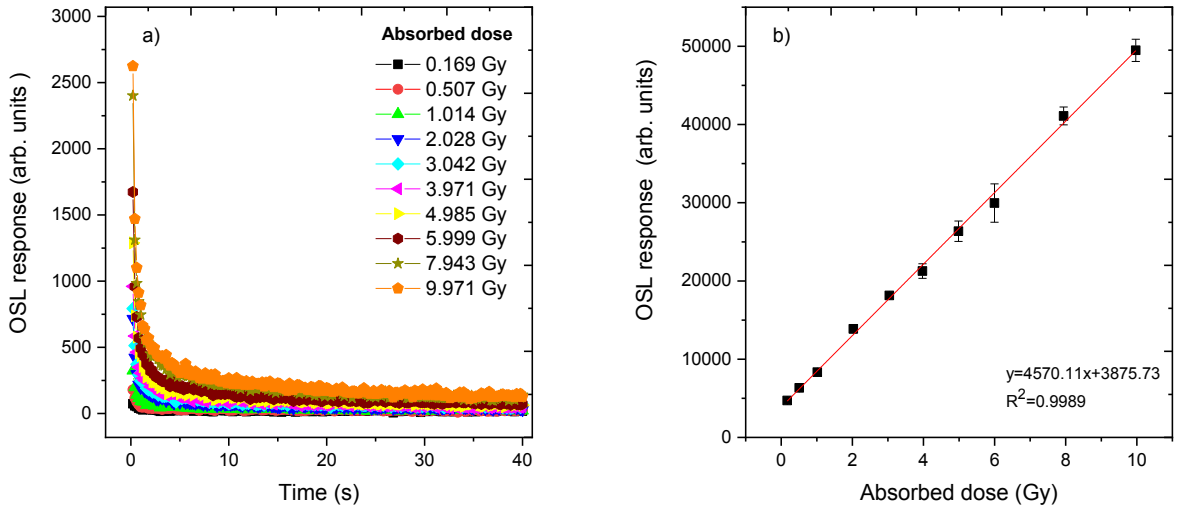

Figure 13. (a) The OSL response of the samples of $CaSO_4$:Mn and (b) as a function of the absorbed dose of beta radiation ($^{90}Sr/^{90}Y$).

3.6.4. OSL fading

Figure 14 shows the OSL signal fading behavior of the $CaSO_4$:Mn sample. The fading test was carried out by exposing several pellets to 169 mGy of beta radiation. The signal loss obtained of 63.6% is given by the ratio between the OSL signal from the stored sample (after 28 days) and the signal from the same pellets read immediately after irradiation. The samples exhibited a strong fading, but well below TL fading.

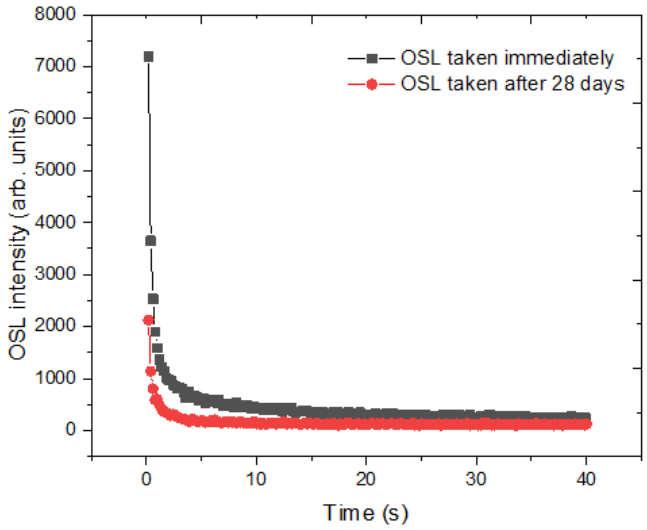

Figure 14. OSL decay curve for $CaSO_4$:Mn samples, read immediately after irradiation at 169 mGy and after 28 days.

3.6.7. Minimum detectable dose

The minimum detectable dose (MDD) of $CaSO_4$:Mn pellets was estimated by calculating the average and standard deviation of the TL/OSL signal of the samples treated at 400°C for 1h and those not irradiated. As shown in Table 3, the values obtained for the minimum detectable dose were: 4.95mGy and 189.8mGy for TL technique and OSL technique, respectively. The estimated value of its MDD is important in low dose measurements where the dosimeter signal is almost equal to the background signal.

Table 3. MDD values for $CaSO_4$:Mn and their uncertainties for the TL and OSL techniques.

Luminescent technique	$\bar{B}$ (arb. units)	$\sigma_{\bar{B}}$ (arb. units)	f_c (mGy/ arb. units)	MDD (mGy)
TL	2414.3	287.4	0.0015	4.95±0.03
OSL	6767.5	100.7	0.0268	189.83±0.09

3.6.8. Correlation between the TL and OSL emissions

Figure 15 (a) shows the TL glow curve of the $CaSO_4$:Mn samples without previous OSL stimulation (black line) and TL with previous OSL stimulation (red line). The previous OSL measurements of the samples significantly reduced the TL signal, by approximately 30.75%. In this case, it is correct to affirm that the OSL signal is correlated to the TL peak. When comparing other materials produced by the slow evaporation route, the $CaSO_4$:Mn presented a TL signal with the lowest photoionization cross section in relation to $CaSO_4$:Tm and $CaSO_4$:Tm,Ag [Junot *et al.*, 2019], $CaSO_4$:Tb [Silva *et al.*, 2020] and $CaSO_4$:Mn,Tb [Silva *et al.*, 2022]. For the same photon flux of the light source, a low photoionization cross section of the trap denotes a low probability of release of the trapped electrons after an optical stimulation, which results in a less intense decay of the OSL signal [Valença *et al.*, 2018].

Figure 15 (b) shows the OSL exponential decay without previous TL stimulation (black line) and OSL with previous TL stimulation (red line). It was also observed that the previous TL measurements of the samples significantly reduced the OSL signal, causing the reduction of the OSL signal to background levels. This indicates that the optically active traps are easily emptied by thermal stimulation [Junot *et al.*, 2019].

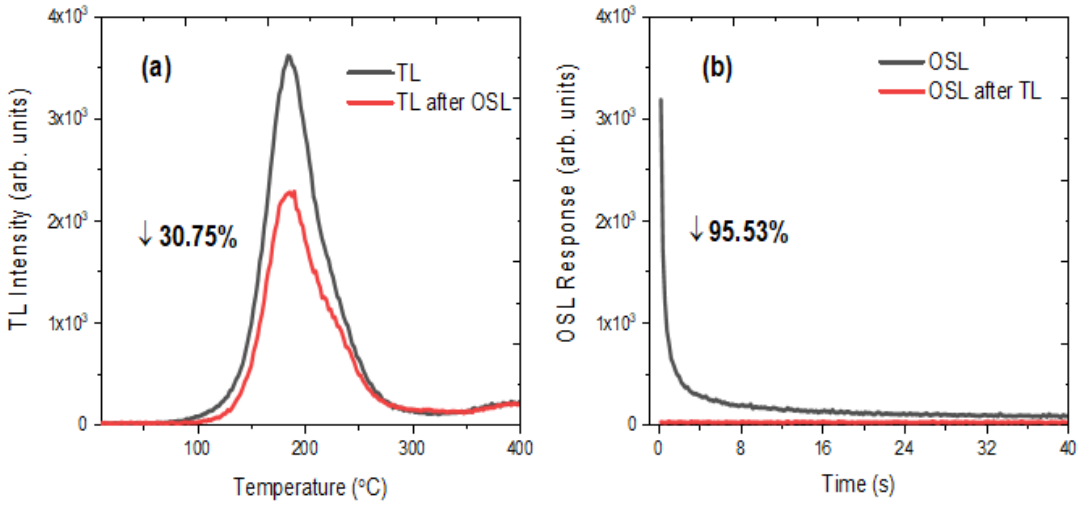

Figure 15. Correlation between the TL and OSL emissions of the $CaSO_4$:Mn samples (a) obtained from consecutive luminescent measurements TL→ OSL and (b) OSL → TL.

4.- CONCLUSIONS

Although the $CaSO_4$:Mn has been left out by the scientific community due to its low temperature peak and strong fading of its TL signal, these characteristics can be partially circumvented by applying a suitable preparation method. In this work manganese doped $CaSO_4$ were synthesized by an adaptation of the slow evaporation route, and the obtained powders were calcined at 600°C for 2 h. The X-ray diffraction analyses showed that the phosphor was efficiently synthesized, since the diffraction peaks agree with those of $CaSO_4$ anhydrite (ICDD 00-037-1496) pattern to a crystal of orthorhombic symmetry. SEM images showed irregular grain morphology with quite agglomeration grains and average crystal dimensions of <150 µm. The results for the PL and TL emission spectra confirmed the presence Mn^{2+} ions in the crystal matrix, once the emission band fits with the characteristic line of the Mn^{2+} emission features, ascribed to the $^6A_1 \rightarrow {}^4T_1$ transition. The thermal behaviors by thermogravimetric analysis (TGA) showed that the temperature used for sintering the pellets at 450°C for 1 h is adequate since there is an insignificant

weight loss. A dosimetric analysis showed that $CaSO_4$:Mn for different heating rates presented the glow curve with a single typical peak and trapping centers located between 0.83 eV and 1.07 eV. The order of kinetics was found to be between one and two, indicating the existence of a general order of kinetics in the TL process. $CaSO_4$:Mn presented a higher TL sensitivity to radiation than CaF_2:Dy, CaF_2:Mn and $CaSO_4$:Dy. The samples also showed an adequate OSL decay curve, with a predominance of a fast decay component. All samples presented properties useful for dosimetric purposes, linearity of the luminescent signals, when irradiated with doses between 169 mGy and 10 Gy, good reproducibility, lowest detectable doses for the OSL and TL signals, on the order of mGy; besides that, they present a significantly fading below those reported in the literature. After 28 days, the TL glow curve showed a 75% fading of its original value, and for the OSL decay curve the signal loss obtained was of 63.6%.

Acknowledgments

The authors thank the Brazilian agencies Comissão Nacional de Energia Nuclear (CNEN), Coordenação de Aperfeiçoamento de Pessoal de Nível Superior - CAPES (Project 88881.157892/2017-01), Conselho Nacional de Desenvolvimento Científico e Tecnológico - CNPq (Projects: 427010/2016-0, 308090/2016-0, 165609/2020-6, 305142/2021-6, 160306/2019-1 and 466512/2018-5), Fundação de Amparo a Pesquisa do Estado de São Paulo – FAPESP (Project 2018/05982-0) and MultiLab (Multi-User Physics Laboratories) and CLQM (Center of Multi-users Chemistry Laboratories) from Federal University of Sergipe for the analysis support.

REFERENCES

Bahl, S., Kumar, V., Bihari, R.R., Kumar, P., 2017. Investigations of OSL properties of $CaSO_4$:Mn phosphor exposed to gamma and beta radiations, J. Lumin. 181,36–43. https://doi.org/10.1016/j.jlumin.2016.09.004

Chen, R., McKeever, S.W.S., 1997. Theory of Thermoluminescence and Related Phenomena. World Scientific, New Jersey.

Du, A., Du, Q., Liu, X., Yang, Y., Xia, C., Zou, J., Li, J., 2021. Ce: YAG transparent ceramics enabling high luminous efficacy for high-power LEDs/LDs. J. Inorg. Mater., 36(883). 10.15541/jim20200727

ISO 12794, 2000. Nuclear energy–radiation protection–individual thermoluminescence dosemeters for extremities and eyes. International Organization for Standardization, Geneva.

Junot, D. O., Barros, J. P., Caldas, L. V. E., Souza, D. N., 2016. Thermoluminescent analysis of $CaSO_4$:Tb,Eu crystal powder for dosimetric purposes, Radiat. Meas. 90, 228–232. https://doi.org/10.1016/j.radmeas.2016.01.020

Junot, D. O., Santos, A. G., Antonio, P. L., Rezende, M. V., Souza, D. N., Caldas, L. V. E., 2019. Dosimetric and optical properties of $CaSO_4$: Tm and $CaSO_4$: Tm, Ag crystals produced by a slow evaporation route. J. Lumin., 210, 58-65. https://doi.org/10.1016/j.jlumin.2019.02.005

Kadari, A., Kadri, D., 2015. New numerical model for thermal quenching mechanism in quartz based on two-stage thermal stimulation of thermoluminescence model, Arab. J. Chem. 8,798-802. https://doi.org/10.1016/j.arabjc.2013.05.027

Kadari, A., Mahi, K., Mostefa, R., Badaoui, M., Mameche, A., & Kadri, D., 2016. Optical and structural properties of Mn doped CaSO4 powders synthesized by sol-gel process. J. Alloys Compd. 688, 32-36. https://doi.org/10.1016/j.jallcom.2016.07.040

Lin, S., Lin, H., Ma, C., Cheng, Y., Ye, S., Lin, F., Wang, Y., 2020. High-security-level multi-dimensional optical storage medium: nanostructured glass embedded with LiGa5O8: Mn^{2+} with photostimulated luminescence. Light Sci. Appl. 9, 1-10. https://doi.org/10.1038/s41377-020-0258-3

Liu, X., Wang, Y., Li, X., Yi, Z., Deng, R., Liang, Liu, X., 2017. Binary temporal up conversion codes of Mn^{2+}-activated nanoparticles for multilevel anti-counterfeiting. Nat. Commun., 8, 899. https://doi.org/10.1038/s41467-017-00916-7

Luchechko, A., Zhydachevskyy, Y., Ubizskii, S. Kravets, O., Popov, A.I., Rogulis, U., A. Suchocki, A., 2019. Afterglow, TL and OSL properties of Mn $^{2+}$-doped $ZnGa_2O_4$ phosphor, Sci. Rep. 9,1-8. https://doi.org/10.1038/s41598-019-45869-7

Menon, S. N., Sanaye, S. S., Dhabekar, B. S., Kumar, R., & Bhatt, B. C., 2005. Role of Mn as a co-dopant in $CaSO_4$: Mn, Pr TL phosphor. Radiat. Meas. 39, 111-114. https://doi.org/10.1016/j.radmeas.2004.06.004

Nuraeni, N., Kartikasari, D., Yani, S., Hiswara, E., Haryanto, F., Iskandar, F., & Waris, A., 2019. Thermoluminescence characteristic of CaSO4: Dy on β and γ radiation. J. Phys. Conf. Ser.1248, 012081.

Oberhofer, M., Scharmann, A., 1981. Applied Thermoluminescence Dosimetry, CRC Press, Ispra.

Oberhofer, M., Scharmann, A., 1993. Techniques and management of personnel thermoluminescence dosimetry services. Springer Science & Business Media.

Raghuwanshi, V. S., Harizanova, R., Haas, S., Tatchev, D., Gugov, I., Dewhurst, C., Russel, A., Hoell, A., 2014. Magnetic nanocrystals embedded in silicate glasses studied by polarized SANS. J Non Cryst Solids, 385, 24-29. https://doi.org/10.1016/j.jnoncrysol.2013.10.007

Rani, R. S., Lakshmanan, A. R., Sivakumar, V., Venkatasamy, R., Annalakshmi, O., Jose, M. T., Marimuthu, K. N., 2015. Redox and charge transfer processes and luminescence in $CaSO_4$:Zn,Mn. Radiat. Meas. 76, 1350-4487. https://doi.org/10.1016/j.radmeas.2015.03.001.

Silva, A. M. B., Souza, L. F., Antonio, P. L., Junot, D. O., Caldas, L. V. E., Souza, D. N., 2022. Effects of manganese and terbium on the dosimetric properties of $CaSO_4$.Radiat. Phys. Chem.198,110207.https://doi.org/10.1016/j.radphyschem.2022.110207.

Silva, A. M. B., Silveira, W. S., Matos, T. S., Junot, D. O., Rezende, M. V., Souza, D. N., 2021. Effect of terbium and silver co-doping on the enhancement of photoluminescence in $CaSO_4$ phosphors. Opt. Mater. 111, 110717. https://doi.org/10.1016/j.optmat.2020.110717

Silva, A.M.B., Junot, D.O., Caldas, L.V.E., Souza, D.N., 2020. Structural, optical and dosimetric characterization of $CaSO_4$:Tb, $CaSO_4$:Tb,Ag and $CaSO_4$:Tb,Ag(NP), J. Lumin. 224, 117286. https://doi.org/10.1016/j.jlumin.2020.117286

Song, E., Ye, S., Liu, T., Du, P., Si, R., Jing, X., Ding, S., Peng, M., Zhang, Q., Wondraczek, L., 2015. Tailored Near-Infrared Photoemission in Fluoride Perovskites through Activator Aggregation and Super-Exchange between Divalent Manganese Ions. Adv. Sci., 2,1500089. https://doi.org/10.1002/advs.201500089

Valença, J. V., Silva, A. C., Dantas, N. O., Caldas, L. V., d'Errico, F., Souza, S. O., 2018. Optically stimulated luminescence of the 20Li2CO3 – (X)K2CO3 – (80 -X)B2O3 glass system, J. Lumin. 200, 248-253. https://doi.org/10.1016/j.jlumin.2018.03.060

Wang, X. J., Xie, R. J., Dierre, B., Takeda, T., Suehiro, T., Hirosaki, N., Sekiguchi T., Sun, Z., 2014. A novel and high brightness AlN: Mn^{2+} red phosphor for field emission displays. Dalton Trans., 43(16), 6120-6127. https://doi.org/10.1039/C3DT53532K

Watanabe, K., 1951. Properties of $CaSO_4$:Mn phosphor under vacuum ultraviolet excitation, Phys. Rev. 83, 785–791. https://doi.org/10.1103/PhysRev.83.78

Yamashita, T., Sakai, K., Kitamura, S., 1970. Calcium sulfate activated by lead and manganese for thermoluminescence dosimetry. J. Nucl. Sci. 7, 105-110. DOI:10.1080/18811248.1970.9734651

Zahedifar, M., Mehrabi, M., Harooni, S., 2011. Synthesis of $CaSO_4$:Mn nanosheets with high thermoluminescence sensitivity. Appl. Radiat. Isot. 69, 1002-1006. https://doi.org/10.1016/j.apradiso.2011.01.036

Zhou, C., Song, J., Zhou, L., Zhong, L., J. Liu, J., Qi, Y., 2015. Greener synthesis and optimization of highly photoluminescence Mn^{2+}-doped ZnS quantum dots. J. Lumin. 158, 176-180, 10.1016/j.jlumin.2014.09.053